Lysosomal biogenesis and function is critical for necrotic cell death in *Caenorhabditis elegans*

Marta Artal-Sanz, Chrysanthi Samara, Popi Syntichaki, and Nektarios Tavernarakis

Institute of Molecular Biology and Biotechnology, Foundation for Research and Technology, Heraklion 71110, Crete, Greece

Necrotic cell death is defined by distinctive morphological characteristics that are displayed by dying cells (Walker, N.I., B.V. Harmon, G.C. Gobe, and J.F. Kerr. 1988. *Methods Achiev. Exp. Pathol.* 13:18–54). The cellular events that transpire during necrosis to generate these necrotic traits are poorly understood. Recent studies in the nematode *Caenorhabditis elegans* show that cytoplasmic acidification develops during necrosis and is required for cell death (Syntichaki, P., C. Samara, and N. Tavernarakis. 2005. *Curr. Biol.* 15:1249–1254). However, the origin of cytoplasmic acidification remains elusive. We show that the alkalization of endosomal and lysosomal compartments ameliorates necrotic cell death triggered by diverse stimuli. In addition, mutations in genes that result in altered lysosomal biogenesis and function markedly affect neuronal necrosis. We used a genetically encoded fluorescent marker to follow lysosome fate during neurodegeneration in vivo. Strikingly, we found that lysosomes fuse and localize exclusively around a swollen nucleus. In the advanced stages of cell death, the nucleus condenses and migrates toward the periphery of the cell, whereas green fluorescent protein–labeled lysosomal membranes fade, indicating lysosomal rupture. Our findings demonstrate a prominent role for lysosomes in cellular destruction during necrotic cell death, which is likely conserved in metazoans.

Introduction

Previous studies implicate necrotic cell death in devastating human pathologies such as stroke and neurodegenerative diseases (Walker et al., 1988; Martin, 2001). In *Caenorhabditis elegans*, specific mutations in several genes that encode ion channel subunits and regulators trigger the degeneration of specific sets of neurons (for review see Syntichaki and Tavernarakis, 2003). Dying neurons exhibit macroscopic and ultrastructural characteristics that are reminiscent of the excitotoxic neuronal death that occurs during stroke in mammals (Hall et al., 1997; Lee et al., 1999; Nicotera et al., 1999). Thus, vertebrates and *C. elegans* share a death mechanism that involves the hyperactivation of ion channels. These observations are consistent with the hypothesis that a threshold of ion influx is needed to initiate the degenerative process.

Perturbation of cellular ionic homeostasis contributes decisively to necrotic neuronal death (Syntichaki and Tavernarakis, 2003). In addition to ion homeostasis, intracellular pH has emerged as an important modulator of necrosis in *C. elegans*. Cytoplasmic acidification develops during necrosis, whereas the vacuolar H^+-ATPase, which is a pump that acidifies lysosomes, is required downstream of cytoplasmic calcium overload to promote necrotic cell death (Syntichaki et al., 2005).

Interestingly, similar acidosis accompanies necrotic cell death after stroke in mammals (Sapolsky et al., 1996; Nicotera et al., 1999). Moreover, the examination of postmortem human brains associates neuronal pH alterations with several pathological and neurodegenerative states (Li et al., 2004). Investigations in both nematodes and mammals converge to implicate specific calpain and aspartyl proteases (cathepsins) in the execution of necrotic cell death (Syntichaki et al., 2002; Yoshida et al., 2002). Calpain proteases are normally dependent on calcium for activation, whereas aspartyl proteases require a highly acidic environment for full activity and are primarily confined to lysosomes and other acidic endosomal compartments (Ishidoh and Kominami, 2002; Goll et al., 2003). Studies in primates indicate that damage to the lysosomal membrane is inflicted enzymatically by activated calpains. Calpains localize to lysosomal membranes after the onset of ischemic episodes, with subsequent spillage of cathepsins to the cytoplasm (Yamashima et al., 2003). This observation led to the formulation of the "calpain–cathepsin hypothesis," whereby the calcium-mediated activation of calpains results in the rupture of lysosomes and leakage of killer cathepsins that eventually dismantle the cell (Yamashima et al., 1998; Yamashima, 2000, 2004). Although these observations collectively indicate that lysosomes participate actively in the process of cell death, their contribution is poorly understood.

Correspondence to Nektarios Tavernarakis: tavernarakis@imbb.forth.gr

We examined the role of lysosomes in a well defined model of necrotic cell death in the nematode. We show that the alkalization of endosomal and lysosomal compartments protects against necrotic cell death that is induced by mutations in several ion channels, as well as by prolonged hypoxia. We investigated the effect of mutations that alter lysosome biogenesis in necrotic cell death and found that mutations resulting in the accumulation of large lysosomes exacerbate necrosis, whereas mutations that impair lysosome biogenesis are protective. Conditions that counterbalance intracellular acidification enhance suppression of neurodegeneration by aspartyl protease deficiency, indicating that aspartyl proteases are activated by low pH conditions, which develop during necrosis. By monitoring lysosomes during necrosis in vivo, we show that lysosomes coalesce around the nucleus and dramatically enlarge during the early and intermediate stages of necrosis, although, ultimately, lysosomal definition is lost. Together, these results point to a decisive role for lysosomes in the execution of necrotic cell death.

Results

Alkalization of endosomal and lysosomal compartments protects against necrotic cell death

Recent data suggests that vacuolar H^+-ATPase–mediated intracellular acidification is required downstream of cytoplasmic calcium overload to promote necrotic cell death, plausibly by enhancing the activity of the low pH–dependent proteases that dismantle the cell (Syntichaki et al., 2005). To emulate impaired lysosomal acidification in degenerating neurons, we treated animals expressing a neurotoxic *gain-of-function* (*gf*) *mec-4(d)* allele encoding a hyperactive ion channel subunit that is normally required for mechanosensation with NH_4Cl and acridine orange. These lysotropic weak bases are known to accumulate in lysosomes and other acidic subcellular compartments, neutralizing their pH (Oka and Futai, 2000). Treatment ameliorated degeneration of the six touch receptor neurons of *mec-4(d)* mutant animals (Fig. 1 A). Similarly, cell death inflicted by the toxic *deg-3(d)* allele, encoding a hyperactive acetylcholine receptor calcium ion channel, or by overexpression of the hyperactivated $G\alpha_s$(Q227L) variant (α_s(*gf*)) was also suppressed after treatment with NH_4Cl and acridine orange (Fig. 1 A). We assessed cell survival by scoring for expression of a touch receptor–specific *mec-4*::GFP reporter fusion in adult animal neurons. Fluorescent neuron number increased after treatment with alkalizing agents in adult *mec-4(d)* mutant animals (309 ± 19 NH_4Cl and 192 ± 13 acridine orange vs. 176 ± 11 fluorescent neurons in untreated *mec-4(d)* mutants; n = 100; P < 0.001, unpaired t test).

Prolonged hypoxia, which is a condition of low oxygen availability that emerges during ischemia and stroke, induces necrotic cell death in the nematode (Scott et al., 2002). We examined the effect of alkalization in hypoxia-induced cell death. Nematodes were treated with sodium azide, which inhibits complex IV (cytochrome *c* oxidase) of the respiratory chain and simulates hypoxia. Treatment with NH_4Cl and acridine orange reduced the hypoxic death of wild-type animals (Fig. 1 B).
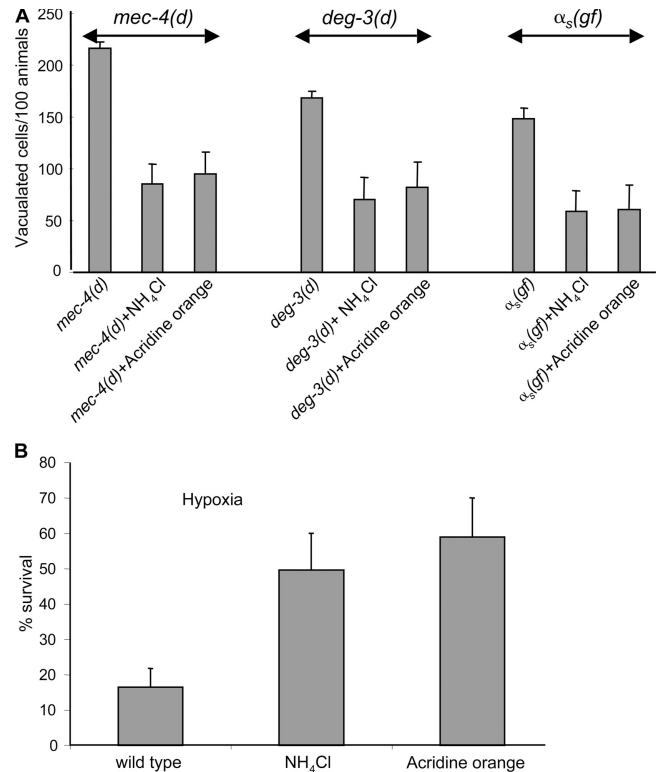

Figure 1. **Alkalization of endosomal compartments by weak bases protects against necrotic cell death.** (A) Degenerating touch receptor neurons in *mec-4(d)* and PVC interneurons in *deg-3(d)* and α_s(*gf*) in untreated animals or animals treated with NH_4Cl and acridine orange. n > 150. P < 0.001, unpaired t test. (B) The effects of alkalizing agents on hypoxic death. The graph shows the percentage of animals that survived near-lethal treatment with sodium azide. n > 200. P < 0.001; unpaired t test. Error bars represent the SD of the mean.

We considered whether suppression of necrosis is an indirect effect of probable alterations in animal growth and development caused by alkalizing agents. We assayed developmental timing after egg hatching and past the L1 stage, which is where we assayed for cell death. We also assayed for animal locomotion, pharyngeal pumping, and defecation. Treatment with NH_4Cl and acridine orange, at the concentrations and under the conditions used, does not result in any discernible defects in animal growth and development that could influence the course of necrotic cell death. We conclude that dependence on acidified intracellular compartments is a common denominator of necrotic cell death triggered by diverse stimuli.

Altered lysosomal biogenesis affects necrosis

To further evaluate the lysosomal role in necrotic cell death, we examined mutants defective in lysosomal biogenesis. We examined necrosis in *cup-5 loss-of-function* (*lf; ar465*) mutant animals. Cells of *cup-5(lf)* mutants contain increased numbers of enlarged acidic lysosomes. *cup-5* encodes the *C. elegans* mucolipin-1 homologue that is implicated in mucolipidosis type IV, which is a lysosomal storage disease that results in severe developmental neuropathology in humans (Fares and Greenwald, 2001; Hersh et al., 2002; Treusch et al., 2004). Neurodegeneration
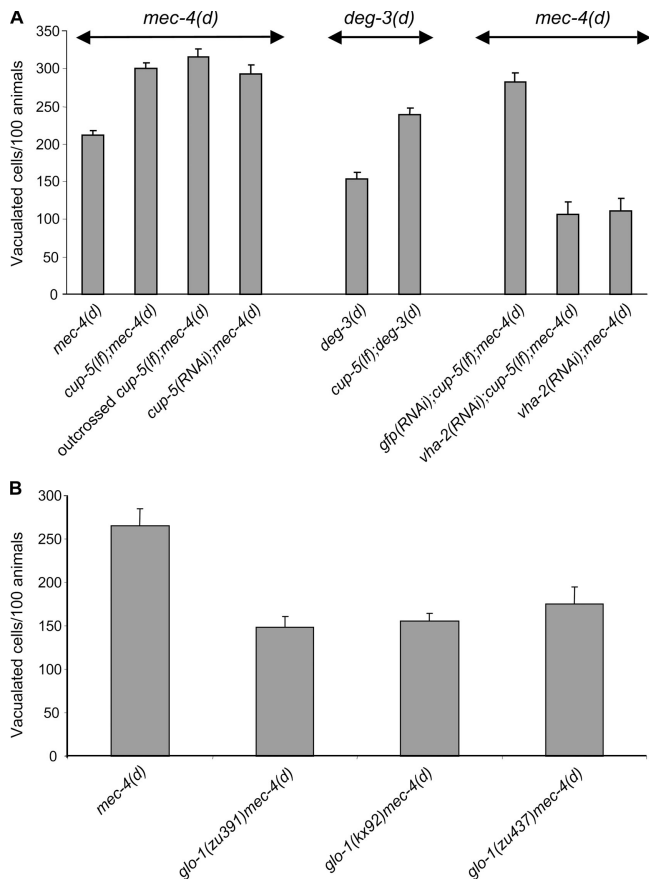
Figure 2. **Effect of lysosomal biogenesis mutants on necrotic cell death.** (A) Neurodegeneration is enhanced in a *cup-5(lf)* genetic background, where the lysosomal system is expanded. This enhancement is suppressed by vacuolar H⁺-ATPase deficiency. Degenerating neurons in *mec-4(d)*, *cup-5(lf);mec-4(d)*, outcrossed *cup-5(lf);mec-4(d)*, *cup-5(RNAi);mec-4(d)*, *deg-3(d)*, and *cup-5(lf);deg-3(d)* animals. Knockdown of *cup-5* by RNAi also enhances *mec-4(d)*–induced neurodegeneration. $n > 250$. $P < 0.005$; unpaired t test. (B) Neurodegeneration is suppressed by three different *glo-1* mutant alleles, where lysosomal biogenesis is defective. Degenerating neurons in *mec-4(d)*, *glo-1(zu391)mec-4(d)*, *glo-1(kx92)mec-4(d)*, and *glo-1(zu437)mec-4(d)* animals. $n > 350$. $P < 0.005$, unpaired t test. Error bars represent the SD of the mean.

inflicted by *mec-4(d)* and *deg-3(d)* is exacerbated in *cup-5(lf)* mutants (Fig. 2 A). We confirmed the reduced cell survival by scoring for expression of a touch receptor–specific *mec-4*::GFP reporter fusion in adult animal neurons. Fluorescent neuron number decreased in *cup-5(lf);mec-4(d)* double mutants, compared with *mec-4(d)* mutant animals (109 ± 16 *cup-5(lf);mec-4(d)* versus 176 ± 11 fluorescent neurons in *mec-4(d)* mutants; $n = 150$; $P < 0.001$, unpaired t test).

In addition, *cup-5(lf)* mutants showed increased sensitivity to hypoxia compared with wild type ($16.5 \pm 5.3\%$ wild-type survival versus $5.3 \pm 4.1\%$ *cup-5(lf)* animal survival. $n > 200$; $P < 0.005$, unpaired t test). Knockdown of *vha-2*, which encodes for a subunit of the vacuolar H⁺-ATPase, by RNAi in *cup-5(lf);mec-4(d)* double mutants abolished *cup-5(lf)*–mediated enhancement of cell death (Fig. 2 A). This suggests that the enhanced cell death observed in *cup-5(lf);mec-4(d)* double mutants is caused by increased lysosome-mediated acidification. To confirm the effect of *cup-5* deficiency on cell death, we out-

crossed *cup-5(lf)* mutant animals in an effort to minimize the possibility that the effects on neurodegeneration we observed were caused by unlinked spurious mutations in the genetic background of the *cup-5(lf)* allele. Furthermore, we used RNAi to specifically target *cup-5*. Both outcrossed *cup-5(lf)* derivatives and RNAi-mediated knockdown of *cup-5* resulted in enhanced *mec-4(d)*–induced neurodegeneration (Fig. 2 A).

In a reciprocal approach, we examined necrosis in *glo-1(lf)* mutants. The *glo-1* gene encodes a predicted Rab GTPase that is similar to proteins implicated in the biogenesis of specialized lysosome-related organelles (Hermann et al., 2005). *glo-1* mutant alleles were recovered in a screen aimed at identifying genes involved in the formation of birefringent gut granules, which are lysosome-related organelles (Hermann et al., 2005). *glo-1(lf)* mutants are defective in the biogenesis of lysosome-related gut granules, show little or no staining with lysosomal markers, and lack detectable expression of the vacuolar H⁺-ATPase subunits VHA-17 and VHA-11 in intestinal precursor cells (Hermann et al., 2005). We found that all three *glo-1(lf)* alleles ameliorate necrotic cell death triggered by *mec-4(d)* (Fig. 2 B). This suggests that the reduced number of lysosomes in touch receptor neurons of *glo-1(lf)mec-4(d)* double mutants results in reduced intracellular acidification and, consequently, in reduced necrotic cell death.

Suppression of necrosis by aspartyl protease deficiency is enhanced by conditions that impede lysosome-mediated intracellular acidification

Specific calpain and aspartyl proteases are implicated in the execution of necrotic cell death in both nematodes and mammals (Syntichaki et al., 2002; Yoshida et al., 2002), and the importance of calpain and aspartyl protease activation in acute cell injury and necrotic cell death triggered by calcium influx has been previously established (for review see Artal-Sanz and Tavernarakis, 2005). Calpain proteases become activated upon the abrupt increase of intracellular calcium that occurs in response to diverse necrosis-initiating stimuli, whereas aspartyl proteases function optimally under the highly acidic conditions present in the lumen of lysosomes and other acidic endosomal compartments (Ishidoh and Kominami, 2002; Goll et al., 2003).

We assessed the effect of lysosome-mediated intracellular acidification on the requirement for aspartyl proteases in necrosis. *cad-1(j1)* mutants maintain aspartyl protease activity that is 90% lower than in wild-type animals (Jacobson et al., 1988). *mec-4(d)*–induced neurodegeneration is attenuated in *cad-1(j1);mec-4(d)* double-mutant strains (Syntichaki et al., 2002). RNAi-mediated knockdown of *vha-2* diminishes cell death inflicted by *mec-4(d)* (Fig. 2 B and Fig. 3; Syntichaki et al., 2005). Cell death was further reduced in *cad-1(j1);mec-4(d)* mutant animals by RNAi-mediated knockdown of *vha-2* (Fig. 3). Two aspartyl proteases, ASP-3 and -4, contribute the bulk of protease activity required for neurodegeneration inflicted by diverse genetic insults in *C. elegans* (Syntichaki et al., 2002). Similarly, knockdown of *asp-3* or *asp-4* by RNAi in *vha-12(n2915)mec-4(d)* double mutants augmented survival of the six receptor neurons, compared with single *mec-4(d)*
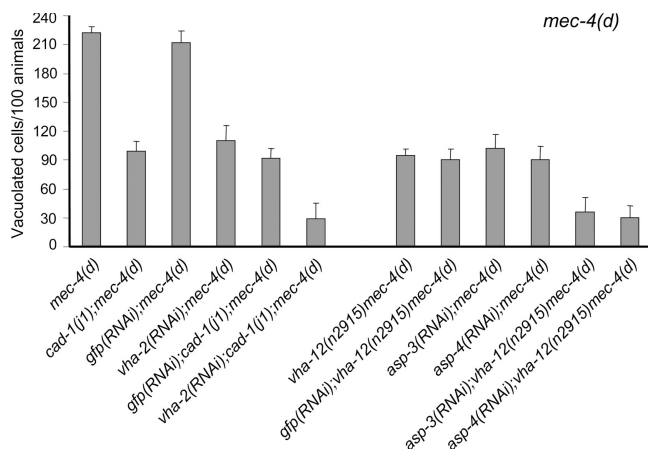
mec-4(d)

Figure 3. **Suppression of necrosis by aspartyl protease deficiency is enhanced by conditions that impede intracellular acidification.** The number of vacuolated touch receptor neurons per 100 L1 stage *mec-4(d)* animals. Bars represent the mean of three independent experiments. $n > 300$. Knockdown of both vacuolar H^+-ATPase and aspartyl protease genes resulted in significantly more extended quenching of neurodegeneration than for any single gene. $P < 0.001$, unpaired *t* test. Efficacy of RNAi was assessed as described in Materials and methods. Error bars represent the SD of the mean.

mutants (Fig. 3). In contrast, reduced V-ATPase activity did not further enhance suppression of necrosis by calpain protease deficiency (Table I). We conclude that suppression of necrosis by aspartyl protease deficiency is enhanced by conditions that impede intracellular acidification.

We considered the contribution of additional cellular pH homeostasis mechanisms in necrosis. Two other major mechanisms have been implicated in cytoplasmic and subcellular organelle pH regulation; first, the sodium–hydrogen exchanger (NHX), and second, the cation transporter P-type ATPase. These mechanisms operate both on the plasma membrane and at the membranes of subcellular organelles, such as mitochondria, to facilitate proton trafficking and pH homeostasis. Multiple *nhx* genes are encoded in the *C. elegans* genome (more than 9 *nhx* isoforms; Nehrke and Melvin, 2002; http://www.wormbase.org). *pmr-1* is the gene encoding the nematode P-type ATPase homologue. Knockdown of *nhx-4, -5,* and *-9*, which are three *nhx* isoforms expressed in neurons, did not alter the extent of neurodegeneration induced by *mec-4(d)* (137 ± 19 *nhx-4(RNAi)mec-4(d)*, 134 ± 16 *nhx-5(RNAi)mec-4(d)*, and 134 ± 21 *nhx-9(RNAi);mec-4(d)* versus 139 ± 14 vacuolated neurons in *mec-4(d)* mutants; $n = 100$). To address the potentially

Table I. **Calpain and V-ATPase activity in necrotic cell death**

Strain	Corpses
mec-4(d)	205 ± 9
gfp(RNAi);mec-4(d)	193 ± 11
clp-1(RNAi);mec-4(d)	96 ± 18
vha-12(n2915)mec-4(d)	112 ± 9
gfp(RNAi);vha-12(n2915)mec-4(d)	101 ± 13
clp-1(RNAi);vha-12(n2915)mec-4(d)	89 ± 16

Suppression of necrosis by calpain protease deficiency is not further enhanced by reduced vacuolar H^+-ATPase activity. Values represent vacuolated touch receptor neurons ($\pm$ SD) per 100 animals at the L1 stage. $n > 250$.

redundant function of these genes in the nervous system, we assayed cell death in animals in which all three isoforms were knocked down by RNAi. We did not observe significant suppression of necrosis in these animals (131 ± 28 *nhx-9(RNAi); nhx-5(RNAi) nhx-4(RNAi)mec-4(d)* versus 139 ± 14 vacuolated neurons in *mec-4(d)* mutants; $n = 100$.). Similarly knockdown of *pmr-1* did not affect necrotic cell death (*pmr-1(RNAi); mec-4(d)*: 141 ± 17, versus 139 ± 14 vacuolated neurons in *mec-4(d)* mutants; $n = 100$). Therefore, neurodegeneration is not affected by compromising these other, nonlysosomal pH homeostasis mechanisms.
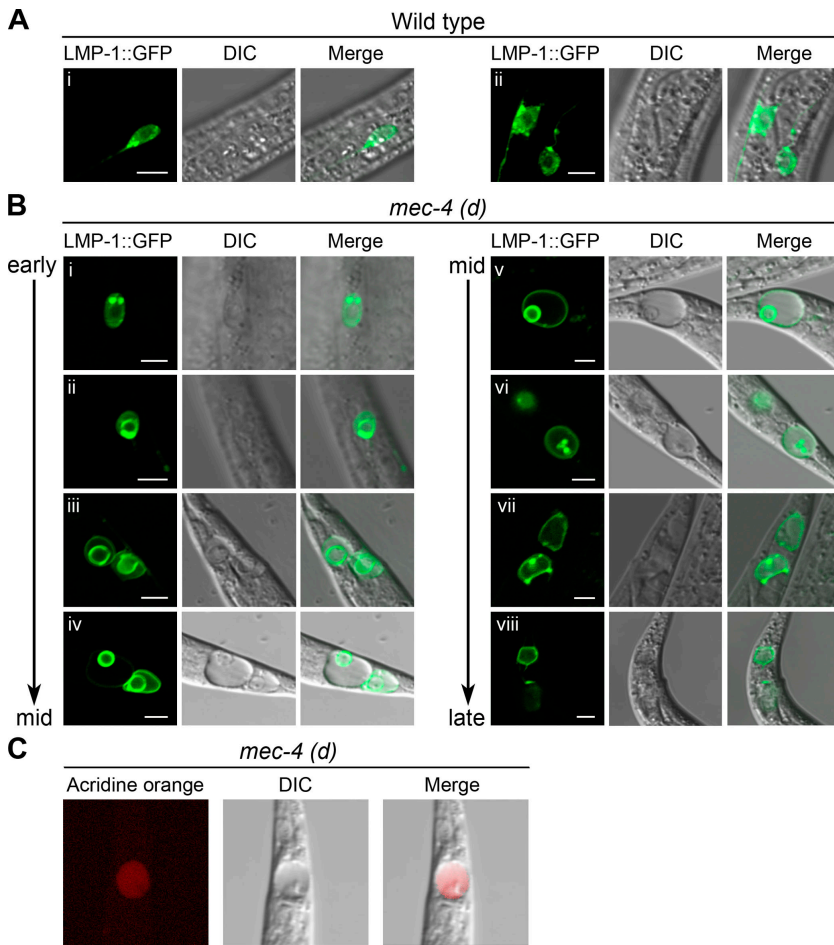
Lysosomal fate during necrosis

The importance of lysosomal membrane permeabilization in cell death has previously been established (Kroemer and Jaattela, 2005). Approaches combining electron microscopy and immunodetection show that calpains concentrate on lysosomal membranes during ischemic stroke in primates (Yamashima, 2000; Yamashima et al., 2003). However, information on lysosome fate and lysosomal system alterations during necrosis in vivo is lacking. We monitored the distribution and morphology of lysosomes in vivo during necrotic cell death in *C. elegans*. To visualize lysosomes and late endosomes, we fused GFP at the COOH terminus of LMP-1, which is the only *C. elegans* protein bearing a lysosomal targeting sequence (GYXXΦ; Φ, large hydrophobic amino acid residue) at its COOH terminus (Kostich et al., 2000). LMP-1 shows similarity to the vertebrate lysosome-associated membrane protein LAMP/CD68 (Kostich et al., 2000; Eskelinen et al., 2003), and it is widely used as a lysosomal marker (Treusch et al., 2004; Hermann et al., 2005; Nunes et al., 2005). We examined lysosomal distribution and morphology in touch receptor neurons of wild-type and *mec-4(d)* animals expressing an LMP-1::GFP fusion.

In the neurons of wild-type animals, lysosomes appear scattered throughout the cytoplasm (Fig. 4 A). In contrast, during the early stages of neurodegeneration, lysosomes enlarge and localize close to the nucleus (Fig. 4 B, i). As neurodegeneration progresses, lysosomes fuse to surround an internally vacuolated structure (Fig. 4 B, ii–viii). This encapsulated vacuole is likely the swollen nucleus of the dying neuron (Hall et al., 1997). To confirm the nuclear origin of the internal vacuole, we performed DAPI staining in *mec-4(d)* animals expressing the LMP-1::GFP fusion protein. As shown in Fig. 5, LMP-1–labeled internal membranes are positive for DAPI staining. In agreement with our observation, elevation of cytosolic Ca^{2+} concentration can induce lysosomal fusion (Bakker et al., 1997). Consistent with previous studies (Hughes and August, 1982; Lippincott-Schwartz and Fambrough, 1986; Hermann et al., 2005), a portion of LMP-1 localizes to the plasma membrane (Fig. 4 B, ii–viii).

Lysosomes remain confined around the distended nucleus during necrotic cell death (Fig. 4 B, ii–v). As neurodegeneration proceeds, the nucleus migrates to the periphery of the cell and condenses (Fig. 4 B, iv–vi). In the advanced stages of neurodegeneration, GFP intensity decreases and lysosomal definition is ultimately lost (Fig. 4 B, vii and viii). Interestingly, a decrease in LMP-1::GFP immunoreactivity is associated with neuronal

A Wild type

LMP-1::GFP | DIC | Merge   LMP-1::GFP | DIC | Merge

i   ii

B *mec-4 (d)*

early

LMP-1::GFP | DIC | Merge   LMP-1::GFP | DIC | Merge

i   mid v

ii   vi

iii   vii

iv   viii

mid   late

C *mec-4 (d)*

Acridine orange | DIC | Merge

Figure 4. **Lysosomal morphology and distribution during neurodegeneration.** (A) Confocal images of wild-type touch receptor neurons expressing a p$_{mec-17}$ LMP-1::GFP transgene. LMP-1::GFP expression, differential interference contrast (DIC), and merged images are shown. Healthy neurons show a scattered and punctate pattern of lysosomal distribution. (i) Wild-type PVM touch receptor neuron. (ii) Wild-type ALM (left and right) touch receptor neurons. (B) Confocal images of PLM touch receptor neurons of *mec-4(d)* animals expressing a p$_{mec-17}$LMP-1::GFP transgene. During the early to middle (mid) stages of degeneration, lysosomes enlarge and appear to coalesce around a swollen nucleus (i–iv). Later on, the nucleus migrates to the periphery of the cell and condenses (iv–vi). At the late stage, no lysosome structure is evident and the vacuolated cell becomes diffusely fluorescent (vii and viii). (C) Acridine orange staining of a middle to late degenerating PLM touch receptor neuron. Acridine orange, DIC, and merged images are shown. Bars, 5 μm.
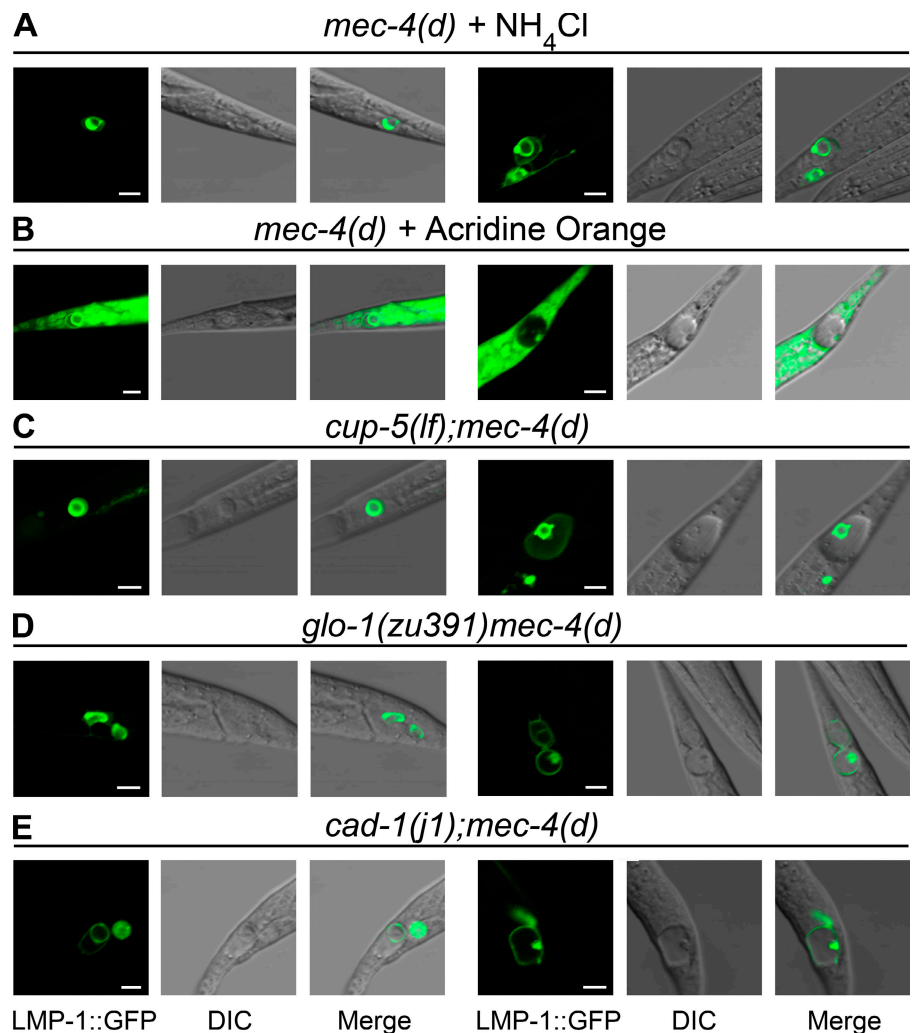
degeneration in mammals (Yamashima et al., 2003). Diffusion of the highly localized GFP staining during the late stages of neurodegeneration indicates lysosome rupture. To further confirm the loss of lysosomal integrity, we stained *mec-4(d)* animals with acridine orange, which is an acidophilic dye that distinctively stains lysosomes. Acridine orange accumulates diffusely in the cytoplasm of neurons during the late stages of necrosis, indicating extensive cytoplasmic acidification (Fig. 4 C). This observation, coupled with the loss of specific LMP-1::GFP localization, suggests that lysosome rupture and the spillage of acidic lysosomal contents mediate cytoplasm acidification during necrosis.

LMP-1::GFP | DAPI | Merge

mec-4(d)

A

B

C
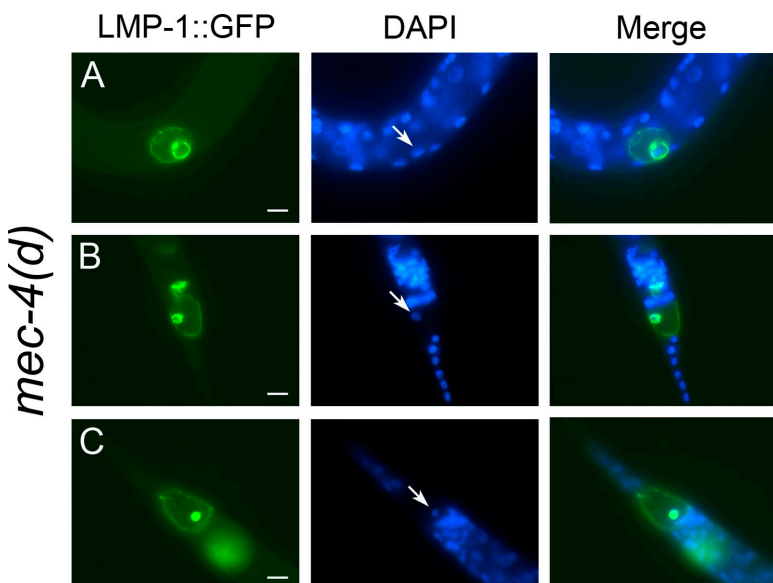
Figure 5. **DAPI staining of *mec-4(d)* animals expressing p$_{mec-17}$LMP-1::GFP.** (A) ALM touch receptor neuron. (B and C) PLM touch receptor neurons. Arrows point to DAPI-positive nuclei of the dying neurons. Bars, 5 μm.

Figure 6. **Perturbation of lysosomal biogenesis, function, and neurodegeneration.** Lysosomal morphology and distribution after treatment with alkalizing agents and in genetic backgrounds affecting lysosomal biogenesis and function. (A and B) Confocal images of PLM touch receptor neurons of *mec-4(d)* animals expressing a p$_{mec-17}$LMP-1::GFP reporter fusion, after alkalization of lysosomal compartments. (A) Images of degenerating neurons after treatment with 5 mM NH$_4$Cl. (B) Degenerating neurons after treatment with 40 μM acridine orange. Nuclei can be seen because, at the concentration used, acridine orange stains DNA. (C–E) Confocal images of PLM touch receptor neurons of *mec-4(d)* animals under different genetic backgrounds that either suppress or enhance necrosis. Double mutants express the same p$_{mec-17}$LMP-1::GFP transgene. (C) Degenerating neurons of *cup-5(lf);mec-4(d)* mutants. Note that vacuoles appear larger. (D) Degenerating neurons of *glo-1(zu391) mec-4(d)* animals. (E) Images of degenerating neurons in *cad-1(j1);mec-4(d)* mutants. LMP-1::GFP expression, differential interference contrast (DIC), and merged images are shown. (left) Early to middle stages of neurodegeneration. (right) Middle to late stages of neurodegeneration. Bars, 5 μm.

A *mec-4(d)* + NH$_4$Cl

B *mec-4(d)* + Acridine Orange

C *cup-5(lf);mec-4(d)*

D *glo-1(zu391)mec-4(d)*

E *cad-1(j1);mec-4(d)*

LMP-1::GFP   DIC   Merge   LMP-1::GFP   DIC   Merge

We investigated whether alkalizing treatments result in altered lysosomal fate. We examined the effects of acridine orange and NH$_4$Cl treatment on LMP-1::GFP distribution in *mec-4(d)* mutants. Although the number of unvacuolated cells with a wild-type pattern of lysosomal distribution increases, vacuolated neurons show the same pattern of lysosomal distribution as *mec-4(d)* animals (Fig. 6, A and B). Thus, reduced acidification does not affect lysosome distribution. Our observations are consistent with findings in animals deficient for the ATP-binding cassette transporter P-glycoprotein-2, which is also expressed in neurons. Acridine orange and Lysotracker red staining is reduced in animals lacking P-glycoprotein 2, indicating defective acidification. Nevertheless, LMP-1::GFP distribution remains unchanged (Nunes et al., 2005). We further examined lysosomes in the different mutant genetic backgrounds that either enhance or suppress necrosis. We generated transgenic animals harboring LMP-1::GFP in *cup-5*, *glo-1*, and the aspartyl protease–deficient *cad-1* mutant background. The number of vacuolated neurons is decreased in *glo-1* and *cad-1* mutants and increased in *cup-5* animals (Figs. 2 and 3). We find that lysosomal morphology and distribution is similar in neurons that do vacuolate and die (Fig. 6, C–E).

Discussion

In this study, we have examined the involvement of lysosomes in necrotic cell death using a well characterized model of neurodegeneration in *C. elegans*. We show that both genetic and pharmacological manipulations that affect lysosomal biogenesis and function modulate necrosis in the nematode. By following lysosome fate during neurodegeneration in vivo, we found that lysosomes fuse and localize exclusively around a swollen nucleus. In the advanced stages of cell death, GFP-labeled lysosomal membranes fade, indicating lysosomal rupture.

What is the cause of lysosomal rupture during necrosis? Interestingly, calcium, which is one of the major upstream death-initiating signals, has been implicated in this process (Zhao et al., 2005). Activated calcium-dependent calpain proteases have been found to localize to disrupted lysosomal membranes in hippocampal neurons of primates after acute ischemia (Yamashima, 2000, 2004), leading to the hypothesis that calpains compromise the integrity of lysosomal membranes and cause leakage of their acidic contents into the cytoplasm. Calpains become activated after the abrupt increase of intracellular calcium concentration that signals the initiation of necrosis (Syntichaki and Tavernarakis, 2002). Excessive calcium influx

through several channels and transporter-mediated routes leads to intracellular calcium overload and concomitant cell death (Lipton and Nicotera, 1998; Nicotera and Bano, 2003). Sodium influx amplifies acute neuronal swelling and facilitates calcium entry through voltage-gated channels and the Na^+/Ca^{2+} exchanger (Sattler and Tymianski, 2000).

Cell injury and death can also be induced by disturbances of calcium homeostasis in the ER (Mattson et al., 2000; Paschen, 2001). The ER is the major calcium storage compartment of the cell. Sequestration of calcium into the ER is mediated by the sarcoendoplasmic reticulum Ca^{2+}-ATPase, and release back to the cytoplasm is controlled by ryanodine, and 1,4,5-inositol trisphosphate receptors (Carafoli, 2002). Within the ER, calcium binds to calcium-binding molecular chaperones such as calreticulin and calnexin (Michalak et al., 1999; Llewellyn et al., 2000). Under conditions of extreme cellular stress, ER calcium stores are rapidly mobilized, boosting the massive increase of intracellular calcium concentration, which signals cell demise (Ferri and Kroemer, 2001). Pharmacological treatments or genetic mutations that inhibit calcium release from the ER have a strong protective effect against necrotic cell death (Yu et al., 2000; Xu et al., 2001). In contrast, treatment with chemicals such as thapsigargin, which promotes the discharge of calcium from intracellular stores by specifically inhibiting the sarcoendoplasmic reticulum Ca^{2+}-ATPase calcium pump, induces necrotic cell death (Takemura et al., 1989; Xu et al., 2001). We hypothesize that generalized osmotic destabilization of the cell during necrosis may also contribute to the bursting of lysosomes.

The exclusive confinement of lysosomes around the nucleus during neurodegeneration may reflect damaged microtubule or actin motors, which mediate the movement of lysosomal organelles (Burkhardt et al., 1997). It is known that calpain proteases contribute to cell death by cleaving essential cytoskeletal proteins of neuronal axons (for review see Artal-Sanz and Tavernarakis, 2005). Therefore, calpains may act on microtubules at early stages of neurodegeneration. However, we cannot rule out the possibility that lysosomes are specifically targeted to the periphery of the nucleus.

We observed that reduction of necrotic cell death by a drop in aspartyl protease activity is enhanced by conditions that counterbalance intracellular acidification. Such synergy between aspartyl proteases and pH indicates that aspartyl proteases become activated by low pH conditions, which develop during necrosis and facilitate cellular destruction. In addition to aspartyl proteases, other proteases that function optimally at low pH may become activated by acidification during necrosis. Such proteases have been implicated in both apoptotic and necrotic cell death (Ferri and Kroemer, 2001). We suggest that preventing acidification suppresses neurodegeneration, in part, by lowering the activity of these enzymes. Alternatively, aspartyl proteases and acidification may independently contribute to cell death. However, to discriminate between these alternatives requires complete elimination of aspartyl protease or vacuolar H^+-ATPase activity, which results in embryonic lethality (Oka and Futai, 2000; Pujol et al., 2001; unpublished data).

The totality of our observations denotes an essential and general role for lysosomes in necrotic cell death induced by various insults. Our study is the first to monitor lysosomal alterations during necrosis in vivo, in any organism. Our findings uncovered novel aspects of the cellular changes that transpire during neurodegeneration in the nematode. Such information could be effectively used toward identifying candidate common intervention targets in an effort to battle numerous pathological conditions in humans. We envision that alterations of lysosomal biogenesis and function by genetic mutations or pharmacological treatments modify the susceptibility of neurons to necrosis. However, once a threshold is exceeded and cell death commences the sequence of events is essentially unaltered.

Materials and methods

Strains and genetics
We used standard procedures for *C. elegans* strain maintenance, crosses, and other genetic manipulations (Brenner, 1974). Nematodes were grown at 20°C. N2 was used as the wild-type strain. The following mutant alleles were used: *mec-4(u231)X*, which is referred to in the text as *mec-4(d)*; *deg-3(u662)V*, which is referred to in the text as *deg-3(d)*; *nuIs5*[p_{glr-1}Gα_s(Q227L)p_{grl-1}GFP], which is referred to in the text as $\alpha_s(gf)$; *arIs37*[p_{myo-3}ssGFP]*I;cup-5(ar465)III;dpy-20(e1282)IV*, which is referred to in the text as *cup-5(lf)*, *cad-1(j1)II*, *glo-1(zu391)X*, *glo-1(Kx92)X*, and *glo-1(zu437)X*. The *glo-1* alleles were provided by G. Hermann (Lewis and Clark College, Portland, OR). The following double and triple mutants were used: *cad-1(j1)II;mec-4(u231)X*, *vha-12(n2915)mec-4(u231)X*, *arIs37*[p_{myo-3}ssGFP]*I;cup-5(ar465)III;dpy-20(e1282)IV;mec-4(u231)X*, *arIs37*[p_{myo-3}ssGFP]*I;cup-5(ar465)III;dpy-20(e1282)IV;deg-3(u662)V*, *glo-1(zu391)-mec-4(u231)X*, *glo-1(kx92)mec-4(u231)X*, and *glo-1(zu437)mec-4(u231)X*.

Plasmids and RNAi
To generate p$_{mec-17}$LMP-1::GFP, we fused GFP at the COOH terminus of the *C. elegans* LMP-1 protein. The translational fusion includes the entire LMP-1 coding sequence lacking the stop codon, a Gly-Ser-Ser-Pro-Gly-Leu-Ala-Lys-Gly-Pro-Lys-Gly linker, and GFP. The resulting chimera was expressed in touch receptor neurons under the control of the *mec-17* promoter. The plasmid carrying the reporter fusion was constructed in two steps. First, the *mec-17* promoter was amplified from N2 genomic DNA with the primers 5′ CGGGATCCGAATCGTCTCACAACTGATCC 3′ and 5′ AACTGCAGG-TGACTACTTGAGACCTG 3′. A 1,900-bp PstI–BamHI fragment was cloned into the promoterless *gfp* vector pPD95.77 (Fire et al., 1990). Second, the LMP-1 coding region was amplified from genomic DNA using the primers 5′ CGGGATCCGACGCTGGCATATCCTTGTCTC 3′ and 5′ CGGGATC-CAATTGAACTATGTTGAAATCG 3′. A BamHI PCR fragment was cloned downstream of the *mec-17* promoter on the pPD95.77 plasmid vector. For RNAi experiments, we used HT115(DE3) *Escherichia coli* bacteria, which were transformed with plasmids that direct the synthesis of double-stranded RNAs corresponding to the genes of interest; they were then fed to animals according to a previously described methodology (Kamath et al., 2001). For *cup-5* RNAi, we used a 1.5-kb PCR-generated fragment derived from the *cup-5* locus using the primers 5′ GGGGTACCCCATGATTTCAGATGTC-TCGC 3′ and 5′ GGGGTACCCCGAATGCAAAGAATGAGAACG 3′. The primers used for *nhx* RNAi constructs are as follows: 5′ GCTCTAGACTC-TTCACTGGCCTGTG 3′ and 5′ CCGCTCGAGATCAGTATGACTGCG 3′ for *nhx-4*, 5′ AACTGCAGTTATGGACGATATCAAC 3′ and 5′ CCGCTCG-AGCCACAAACTTCAGCCAC 3′ for *nhx-5*, and 5′ GCTCTAGATGGTGT-CCTGACTCTTC 3′ and 5′ CCGCTCGAGCTTCCACTCCAGACATC 3′ for *nhx-9*. For *pmr-1* we used the following PCR primers: 5′ AACTGCAGATTG-AAACACTGACATC 3′ and 5′ CCGCTCGAGTACCTGAAACATTCCG 3′. RNAi plasmids for *vha-2*, aspartyl proteases *asp-3* and *asp-4*, and calpain *clp-1* have been previously described (Syntichaki et al., 2002, 2005). We assayed the effectiveness of RNAi by monitoring the expression of full-length GFP reporter fusions. Plasmid vectors for *C. elegans* were provided by A. Fire (Stanford University School of Medicine, Stanford, CA).

Neurodegeneration assays
Degeneration of specific neuron sets in animals bearing *deg-3(d)*, *mec-4(d)*, and $\alpha_s(gf)$ alleles was quantified as previously described (Syntichaki et al., 2002). For alkalization assays, we treated young adult animals with lysotropic alkalizing agents (5 mM NH_4Cl and 40–150 µM acridine orange; Sigma-Aldrich) in liquid cultures supplemented with *E. coli* bacteria for

12 h at 20°C. Neurodegeneration was assayed in the progeny of treated animals at the L1 stage of development. To simulate death-inducing hypoxic conditions, we treated nematodes at the L4 stage of development with sodium azide (0.5 M for 30 min at 20°C; Sigma-Aldrich; adapted with modifications from Scott et al. [2002]). Statistical analysis of data was performed using Excel (Microsoft).

Microscopy
L1 stage *mec-4(d)* animals expressing LMP-1::GFP were stained with 1 µg/ml DAPI for 15 min after methanol fixation. DAPI-stained animals were observed using a 40× objective (Plan-Neofluar; Carl Zeiss MicroImaging, Inc.), NA 0.75, and a 365 ± 12–nm band-pass excitation/397-nm long-pass emission filter set. A microscope was used, and pictures were taken using a camera (AxioPlan and AxioCam, respectively; both Carl Zeiss MicroImaging, Inc.). For LMP-1::GFP imaging, animals were scanned with a 488-nm laser beam, under a confocal microscope (Radiance 2000; Bio-Rad Laboratories), using the LaserSharp 2000 software package (Bio-Rad Laboratories). Images of emission from individual PLM and ALM touch receptor neurons were acquired using a 515 ± 15–nm band-pass filter and a 40× Plan-Neofluar objective, NA 0.75. Acridine orange staining of necrotic cells was done by treating *mec-4(d)* early L1 larvae with 1 µM acridine orange for 20 min. To visualize stained cells, animals were scanned with a 543-nm laser beam. Images of emission from individual touch receptor neurons were acquired using a 590 ± 35–nm band-pass filter. Animals were mounted in a 2% agarose pad in M9 buffer containing 10 mM sodium azide and observed at room temperature. Bright field and epifluorescence images were merged using Photoshop (version 7.0.1; Adobe).

References

Artal-Sanz, M., and N. Tavernarakis. 2005. Proteolytic mechanisms in necrotic cell death and neurodegeneration. *FEBS Lett.* 579:3287–3296.

Bakker, A.C., P. Webster, W.A. Jacob, and N.W. Andrews. 1997. Homotypic fusion between aggregated lysosomes triggered by elevated [Ca2+]i in fibroblasts. *J. Cell Sci.* 110:2227–2238.

Brenner, S. 1974. The genetics of *Caenorhabditis elegans*. *Genetics*. 77:71–94.

Burkhardt, J.K., C.J. Echeverri, T. Nilsson, and R.B. Vallee. 1997. Overexpression of the dynamitin (p50) subunit of the dynactin complex disrupts dynein-dependent maintenance of membrane organelle distribution. *J. Cell Biol.* 139:469–484.

Carafoli, E. 2002. Calcium signaling: a tale for all seasons. *Proc. Natl. Acad. Sci. USA.* 99:1115–1122.

Eskelinen, E.L., Y. Tanaka, and P. Saftig. 2003. At the acidic edge: emerging functions for lysosomal membrane proteins. *Trends Cell Biol.* 13:137–145.

Fares, H., and I. Greenwald. 2001. Regulation of endocytosis by CUP-5, the *Caenorhabditis elegans* mucolipin-1 homolog. *Nat. Genet.* 28:64–68.

Ferri, K.F., and G. Kroemer. 2001. Organelle-specific initiation of cell death pathways. *Nat. Cell Biol.* 3:E255–E263.

Fire, A., S.W. Harrison, and D. Dixon. 1990. A modular set of lacZ fusion vectors for studying gene expression in *Caenorhabditis elegans*. *Gene*. 93:189–198.

Goll, D.E., V.F. Thompson, H. Li, W. Wei, and J. Cong. 2003. The calpain system. *Physiol. Rev.* 83:731–801.

Hall, D.H., G. Gu, J. Garcia-Anoveros, L. Gong, M. Chalfie, and M. Driscoll. 1997. Neuropathology of degenerative cell death in *Caenorhabditis elegans*. *J. Neurosci.* 17:1033–1045.

Hermann, G.J., L.K. Schroeder, C.A. Hieb, A.M. Kershner, B.M. Rabbitts, P. Fonarev, B.D. Grant, and J.R. Priess. 2005. Genetic analysis of lysosomal trafficking in *Caenorhabditis elegans*. *Mol. Biol. Cell.* 16:3273–3288.

Hersh, B.M., E. Hartwieg, and H.R. Horvitz. 2002. The *Caenorhabditis elegans* mucolipin-like gene cup-5 is essential for viability and regulates lysosomes in multiple cell types. *Proc. Natl. Acad. Sci. USA.* 99:4355–4360.

Hughes, E.N., and J.T. August. 1982. Murine cell surface glycoproteins. Identification, purification, and characterization of a major glycosylated component of 110,000 daltons by use of a monoclonal antibody. *J. Biol. Chem.* 257:3970–3977.

Ishidoh, K., and E. Kominami. 2002. Processing and activation of lysosomal proteinases. *Biol. Chem.* 383:1827–1831.

Jacobson, L.A., L. Jen-Jacobson, J.M. Hawdon, G.P. Owens, M.A. Bolanowski, S.W. Emmons, M.V. Shah, R.A. Pollock, and D.S. Conklin. 1988. Identification of a putative structural gene for cathepsin D in *Caenorhabditis elegans*. *Genetics*. 119:355–363.

Kamath, R.S., M. Martinez-Campos, P. Zipperlen, A.G. Fraser, and J. Ahringer. 2001. Effectiveness of specific RNA-mediated interference through ingested double-stranded RNA in *Caenorhabditis elegans*. *Genome Biol.* DOI:10.1186/gb-2000-2-1-research0002.

Kostich, M., A. Fire, and D.M. Fambrough. 2000. Identification and molecular-genetic characterization of a LAMP/CD68-like protein from *Caenorhabditis elegans*. *J. Cell Sci.* 113:2595–2606.

Kroemer, G., and M. Jaattela. 2005. Lysosomes and autophagy in cell death control. *Nat. Rev. Cancer.* 5:886–897.

Lee, J.M., G.J. Zipfel, and D.W. Choi. 1999. The changing landscape of ischaemic brain injury mechanisms. *Nature.* 399:A7–14.

Li, J.Z., M.P. Vawter, D.M. Walsh, H. Tomita, S.J. Evans, P.V. Choudary, J.F. Lopez, A. Avelar, V. Shokoohi, T. Chung, et al. 2004. Systematic changes in gene expression in postmortem human brains associated with tissue pH and terminal medical conditions. *Hum. Mol. Genet.* 13:609–616.

Lippincott-Schwartz, J., and D.M. Fambrough. 1986. Lysosomal membrane dynamics: structure and interorganellar movement of a major lysosomal membrane glycoprotein. *J. Cell Biol.* 102:1593–1605.

Lipton, S.A., and P. Nicotera. 1998. Calcium, free radicals and excitotoxins in neuronal apoptosis. *Cell Calcium.* 23:165–171.

Llewellyn, D.H., S. Johnson, and P. Eggleton. 2000. Calreticulin comes of age. *Trends Cell Biol.* 10:399–402.

Martin, L.J. 2001. Neuronal cell death in nervous system development, disease, and injury. *Int. J. Mol. Med.* 7:455–478.

Mattson, M.P., F.M. LaFerla, S.L. Chan, M.A. Leissring, P.N. Shepel, and J.D. Geiger. 2000. Calcium signaling: its role in neuronal plasticity and neurodegenerative disorders. *Trends Neurosci.* 23:222–229.

Michalak, M., E.F. Corbett, N. Mesaeli, K. Nakamura, and M. Opas. 1999. Calreticulin: one protein, one gene, many functions. *Biochem. J.* 344:281–292.

Nehrke, K., and J.E. Melvin. 2002. The NHX family of Na+-H+ exchangers in *Caenorhabditis elegans*. *J. Biol. Chem.* 277:29036–29044.

Nicotera, P., and D. Bano. 2003. The enemy at the gates. Ca2+ entry through TRPM7 channels and anoxic neuronal death. *Cell.* 115:768–770.

Nicotera, P., M. Leist, and L. Manzo. 1999. Neuronal cell death: a demise with different shapes. *Trends Pharmacol. Sci.* 20:46–51.

Nunes, F., M. Wolf, J. Hartmann, and R.J. Paul. 2005. The ABC transporter PGP-2 from *Caenorhabditis elegans* is expressed in the sensory neuron pair AWA and contributes to lysosome formation and lipid storage within the intestine. *Biochem. Biophys. Res. Commun.* 338:862–871.

Oka, T., and M. Futai. 2000. Requirement of V-ATPase for ovulation and embryogenesis in *Caenorhabditis elegans*. *J. Biol. Chem.* 275:29556–29561.

Paschen, W. 2001. Dependence of vital cell function on endoplasmic reticulum calcium levels: implications for the mechanisms underlying neuronal cell injury in different pathological states. *Cell Calcium.* 29:1–11.

Pujol, N., C. Bonnerot, J.J. Ewbank, Y. Kohara, and D. Thierry-Mieg. 2001. The *Caenorhabditis elegans* unc-32 gene encodes alternative forms of a vacuolar ATPase a subunit. *J. Biol. Chem.* 276:11913–11921.

Sapolsky, R.M., J. Trafton, and G.C. Tombaugh. 1996. Excitotoxic neuron death, acidotic endangerment, and the paradox of acidotic protection. *Adv. Neurol.* 71:237–244.

Sattler, R., and M. Tymianski. 2000. Molecular mechanisms of calcium-dependent excitotoxicity. *J. Mol. Med.* 78:3–13.

Scott, B.A., M.S. Avidan, and C.M. Crowder. 2002. Regulation of hypoxic death in *C. elegans* by the insulin/IGF receptor homolog DAF-2. *Science.* 296:2388–2391.

Syntichaki, P., and N. Tavernarakis. 2002. Death by necrosis: uncontrollable catastrophe, or is there order behind the chaos? *EMBO Rep.* 3:604–609.

Syntichaki, P., and N. Tavernarakis. 2003. The biochemistry of neuronal necrosis: rogue biology? *Nat. Rev. Neurosci.* 4:672–684.

Syntichaki, P., K. Xu, M. Driscoll, and N. Tavernarakis. 2002. Specific aspartyl and calpain proteases are required for neurodegeneration in *C. elegans*. *Nature.* 419:939–944.

Syntichaki, P., C. Samara, and N. Tavernarakis. 2005. The vacuolar H+-ATPase mediates intracellular acidification required for neurodegeneration in *C. elegans*. *Curr. Biol.* 15:1249–1254.

Takemura, H., A.R. Hughes, O. Thastrup, and J.W. Putney Jr. 1989. Activation of calcium entry by the tumor promoter thapsigargin in parotid acinar cells. Evidence that an intracellular calcium pool and not an inositol phosphate regulates calcium fluxes at the plasma membrane. *J. Biol. Chem.* 264:12266–12271.

Treusch, S., S. Knuth, S.A. Slaugenhaupt, E. Goldin, B.D. Grant, and H. Fares. 2004. *Caenorhabditis elegans* functional orthologue of human protein h-mucolipin-1 is required for lysosome biogenesis. *Proc. Natl. Acad. Sci. USA.* 101:4483–4488.

Walker, N.I., B.V. Harmon, G.C. Gobe, and J.F. Kerr. 1988. Patterns of cell death. *Methods Achiev. Exp. Pathol.* 13:18–54.

Xu, K., N. Tavernarakis, and M. Driscoll. 2001. Necrotic cell death in *C. elegans* requires the function of calreticulin and regulators of Ca(2+) release from the endoplasmic reticulum. *Neuron.* 31:957–971.

Yamashima, T. 2000. Implication of cysteine proteases calpain, cathepsin and caspase in ischemic neuronal death of primates. *Prog. Neurobiol.* 62:273–295.

Yamashima, T. 2004. Ca2+-dependent proteases in ischemic neuronal death: a conserved 'calpain-cathepsin cascade' from nematodes to primates. *Cell Calcium.* 36:285–293.

Yamashima, T., Y. Kohda, K. Tsuchiya, T. Ueno, J. Yamashita, T. Yoshioka, and E. Kominami. 1998. Inhibition of ischaemic hippocampal neuronal death in primates with cathepsin B inhibitor CA-074: a novel strategy for neuroprotection based on 'calpain-cathepsin hypothesis'. *Eur. J. Neurosci.* 10:1723–1733.

Yamashima, T., A.B. Tonchev, T. Tsukada, T.C. Saido, S. Imajoh-Ohmi, T. Momoi, and E. Kominami. 2003. Sustained calpain activation associated with lysosomal rupture executes necrosis of the postischemic CA1 neurons in primates. *Hippocampus.* 13:791–800.

Yoshida, M., T. Yamashima, L. Zhao, K. Tsuchiya, Y. Kohda, A.B. Tonchev, M. Matsuda, and E. Kominami. 2002. Primate neurons show different vulnerability to transient ischemia and response to cathepsin inhibition. *Acta Neuropathol. (Berl.).* 104:267–272.

Yu, G., R. Zucchi, S. Ronca-Testoni, and G. Ronca. 2000. Protection of ischemic rat heart by dantrolene, an antagonist of the sarcoplasmic reticulum calcium release channel. *Basic Res. Cardiol.* 95:137–143.

Zhao, H.F., X. Wang, and G.J. Zhang. 2005. Lysosome destabilization by cytosolic extracts, putative involvement of Ca(2+)/phospholipase C. *FEBS Lett.* 579:1551–1556.